RNA (2001), *7*:682–691. Cambridge University Press. Printed in the USA.

Crystal structure of a model branchpoint–U2 snRNA duplex containing bulged adenosines

J. ANDREW BERGLUND,[1] MICHAEL ROSBASH,[2] and STEVE C. SCHULTZ[3]

[1]Department of Chemistry and Biochemistry, University of Colorado, Boulder, Colorado 80309, USA
[2]Howard Hughes Medical Institute, Brandeis University, Waltham, Massachusetts 02254, USA
[3]Department of Math and Sciences, Diné College, Tsaile, Arizona 86556, USA

ABSTRACT

Bulged nucleotides play a variety of important roles in RNA structure and function, frequently forming tertiary interactions and sometimes even participating in RNA catalysis. In pre-mRNA splicing, the U2 snRNA base pairs with the intron branchpoint sequence (BPS) to form a short RNA duplex that contains a bulged adenosine that ultimately serves as the nucleophile that attacks the 5′ splice site. We have determined a 2.18-Å resolution crystal structure of a self-complementary RNA designed to mimic the highly conserved yeast (*Saccharomyces cerevisiae*) branchpoint sequence (5′-*UACUAACG*UAGUA with the BPS italicized and the branchsite adenosine underlined) base paired with its complementary sequence from U2 snRNA. The structure shows a nearly ideal A-form helix from which two unpaired adenosines flip out. Although the adenosine adjacent to the branchsite adenosine is the one bulged out in the structure described here, either of these adenosines can serve as the nucleophile in mammalian but not in yeast pre-mRNA splicing. In addition, the packing of the bulged RNA helices within the crystal reveals a novel RNA tertiary interaction in which three RNA helices interact through bulged adenosines in the absence of any divalent metal ions.

Keywords: pre-mRNA splicing; RNA crystallography; three-helix RNA interaction

INTRODUCTION

Unpaired adenosines are a common feature in RNA structures and are disproportionately represented in certain large folded RNAs such as the 16S ribosomal RNA (Gutell et al., 1985). In the few known RNA tertiary motifs, adenosines are present more often then any of the other 3 nt (Ferre-D'Amare & Doudna, 1999). In addition, single bulged adenosines within otherwise duplex RNAs are catalytically important in pre-mRNA splicing and group II self-splicing introns and allow the antigenomic HDV self-cleaving RNA to avoid a kinetic folding trap (Perrotta et al., 1999).

In nuclear pre-mRNA splicing, introns are removed by a large RNA–protein machine referred to as the spliceosome. The spliceosome is made up of five ribonucleoprotein particles (snRNPs) and approximately 100 non-snRNP associated proteins that specifically recognize introns and catalyze their removal through two transesterification reactions (reviewed in Staley & Guthrie, 1998; Burge et al., 1999). Three regions within the intron itself are involved in the transesterification reactions, the 5′ splice site, the branchpoint sequence (BPS), and the 3′ splice site. In the first transesterification reaction, an adenosine within the BPS attacks the 5′ splice site and in the second reaction the newly freed 5′ exon attacks the 3′ splice site. The BPS is highly conserved in the yeast *Saccharomyces cerevisiae*, with a consensus sequence of UACUAAC, and the branchsite adenosine (underlined) is always used to attack the 5′ splice site (Rymond & Rosbash, 1992; Spingola et al., 1999). In other organisms, such as humans, the consensus BPS is less conserved, and either of the two adjacent adenosines can be used to attack the 5′ splice site (Query et al., 1994). There are also a few examples of the other 3 nt being used as the nucleophile (Adema et al., 1988; Hartmuth & Barta, 1988; Dyhr-Mikkelsen & Kjems, 1995; Zabolotny et al., 1997).

Specific recognition of the BPS occurs several times during splicing. The BPS is first recognized by a single-strand RNA-binding protein referred to as the branchpoint binding protein or splicing factor 1 (Arning et al., 1996; Berglund et al., 1997). The branchsite adenosine is especially important for this interaction, suggesting that it is recognized even in this early event in the splicing pathway. The branchpoint binding protein appears to be involved only in early recognition because it is present only in the early stages of spliceosome

Reprint requests to: Andy Berglund, Campus Box 215, Department of Chemistry and Biochemistry, University of Colorado, Boulder, Colorado 80309, USA; e-mail: Andy.Berglund@Colorado.edu.

formation (Rutz & Séraphin, 1999). Subsequently, U2 snRNP binds and apparently displaces the branchpoint binding protein to form the BPS–U2 snRNP RNA duplex (Parker et al., 1987; Wu & Manley, 1989; Zhuang & Weiner, 1989). In this base-paired structure, the branchpoint adenosine is unpaired and likely bulged out and available for interactions that will position it for nucleophilic attack (Query et al., 1994). A U2 snRNP associated protein U2AF65 has been shown to stabilize the BPS–U2 snRNP RNA duplex (Ruskin et al., 1988; Valcarcel et al., 1996). As the spliceosome reaches the correct conformation for catalysis, other proteins interact with the BPS (MacMillan et al., 1994; Chiara et al., 1996). These includes p14, which specifically crosslinks to the branchsite adenosine (Query et al., 1996) and may play a role in positioning the branchsite adenosine for attack at the 5′ splice site. In addition to these proteins, the RNA of the snRNPs is thought to be involved in forming the catalytic core of the spliceosome and, therefore, is also making intimate contacts with the BPS and branchsite adenosine (reviewed in Nilsen, 1998).

To explore the conformational and structural features at bulged adenosines, we have determined the crystal structure of a self-complementary RNA (5′-**UACUA AC**GUAGUA with the BPS in bold, the branchsite adenosine underlined and the complementary region from U2 snRNP shown in normal font) designed to mimic the BPS–U2 snRNP interaction. The structure shows two different conformations for the bulged adenosine. One of these conformations positions the 2′ OH in a manner amenable to nucleophilic attack and the other does not. In addition, the interactions between the bulged adenosine of two different helices with the minor groove of a third helix in the crystal lattice show how bulged adenosines can be used to form a novel RNA tertiary interaction involving three helices.

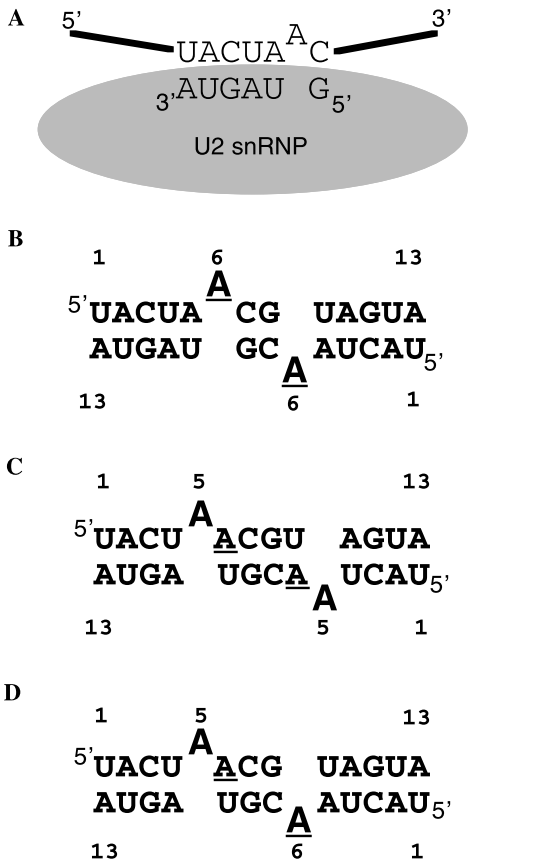

FIGURE 1. Possible secondary structures of the U2 snRNA–BPS helix used for crystallization. **A:** Base pairing between U2 snRNP and the BPS in the spliceosome. **B:** The branchsite adenosines (X6, Y6 underlined) are unpaired. **C:** The adenosines adjacent to the branchsite (X5, Y5) are unpaired and the branchsite adenosines are paired with the uridine. It is this secondary structure observed in the crystal structure. **D:** One branchsite adenosine is unpaired and one adjacent adenosine is unpaired (X5, Y6).

RESULTS AND DISCUSSION

Overview of the structure

The structure of the bulged adenosine RNA helix described here shows how unpaired adenosines can flip out of an RNA helix with only minor structural deviations from an ideal A-form helical conformation. Two different base-pairing schemes are inherent to the BPS–U2 snRNP RNA interaction and because two copies of this interaction are present in the self-complementary RNA crystallized in these studies, three possible secondary structures exist (Fig. 1). The base-pairing scheme shown in Figure 1A leaves the branchsite adenosine unpaired (position 6, underlined) whereas the scheme shown in Figure 1B leaves the preceding adenosine (position 5) unpaired. The third possibility is simply a mixture of the two previous base-pairing schemes (Fig. 1C). In the yeast *S. cerevisiae*, the sixth position is used almost exclusively as the nucleophile in forming the 2′–5′ linkage with the 5′ splice site (Rymond & Rosbash, 1992) whereas in mammalian splicing, either the fifth or sixth position can be effectively used as the nucleophile (Ruskin et al., 1986; Query et al., 1994). The structure we have solved exhibits the base-pairing scheme shown in Figure 1B in which the fifth nucleotide on each strand is unpaired and flipped out of the helix.

The overall three-dimensional structure, shown in Figure 2A,B, shows that the two bulged adenosines adopt two rather different conformations, as will be discussed later. The global conformation of the helix is surprisingly similar to an idealized A-form helix (Fig. 2C) and is not substantially bent, under/over wound, or globally distorted in any other way, but is only locally distorted near the sites of the bulges. This result shows that single bulged nucleotides can easily be accommodated in duplex RNAs without causing major perturbations such as major groove widening or bending of the helix.

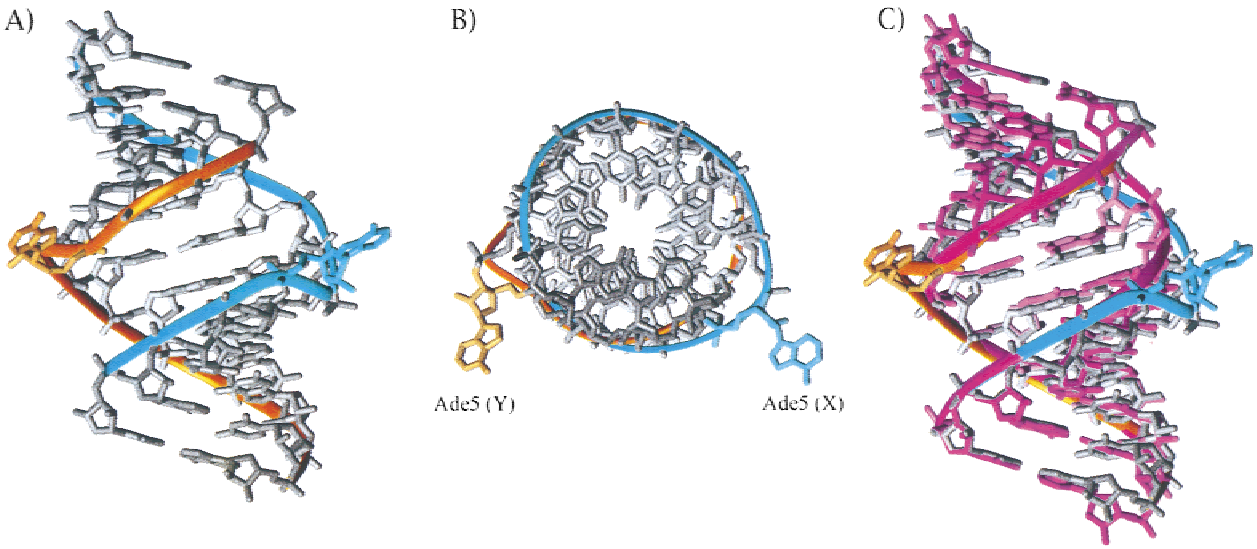

FIGURE 2. Overall structure of the U2 snRNA–BPS RNA and a comparison with A-form RNA. **A:** The backbone and bulged base of the RNA X chain is shown as an aqua ribbon and the other backbone (Y chain) is shown in orange. **B:** The RNA is rotated 90° about the Y axis in comparison to the view in **A**. **C:** Superposition of standard A-form RNA (purple) with the bulged adenosine RNA structure displays the similarity between the two structures.

Helical regions of the structure

The individual nucleotides in the helical region of this RNA all adopt nearly ideal A-form conformations, with the exception of those near the bulged nucleotides. The torsion angles of the sugar–phosphate backbone are plotted versus the nucleotide position in Figure 3. Interestingly, an asymmetry exists in the torsion angles for the two RNA strands, which are hereafter called X and Y. For example, alpha for X7 is 160° whereas alpha for Y7 is 285°, which is more similar to A-form RNA (Fig. 3). This is due to the different conformations of the

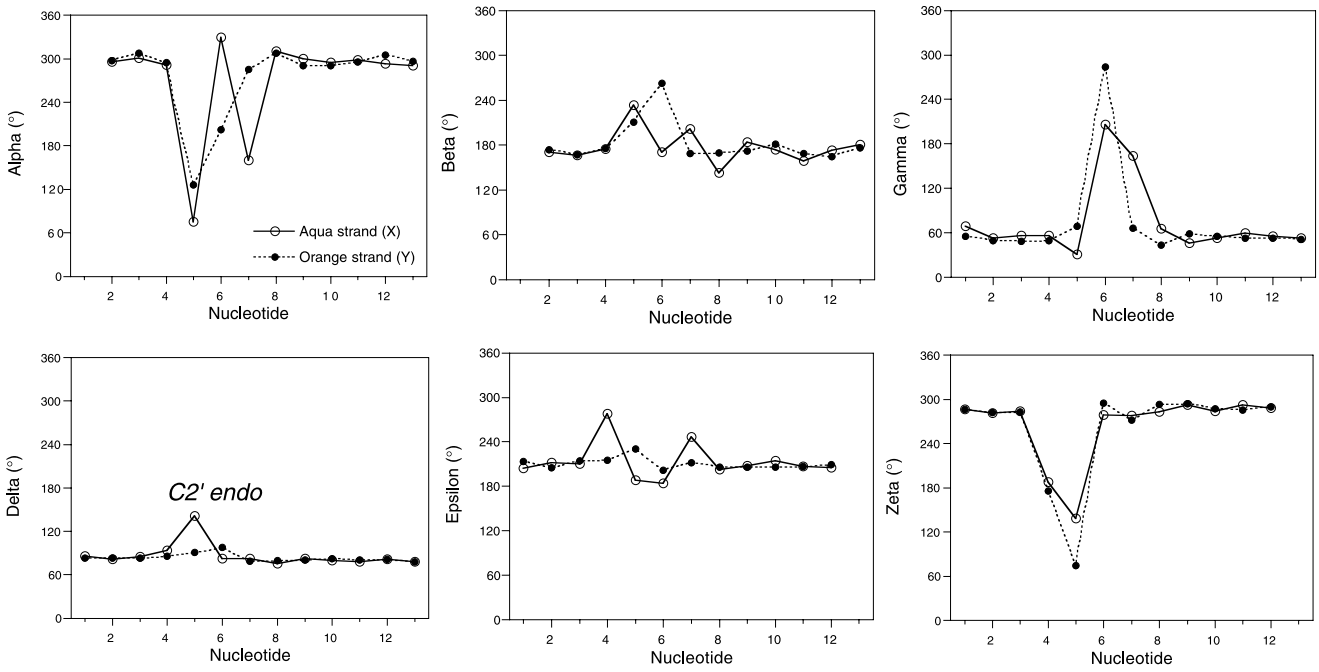

FIGURE 3. Torsion angles for the backbone of the two RNA chains (X, Y). The bulged adenosine RNA helix deviates from A-form RNA in nucleotide positions 4–8. The C2′ endo conformation for the X5 adenosine is labeled in the graph plotting the torsion angle delta versus nucleotide position. These angles were generated using the program Freehelix (Dickerson, 1998).

two bulged adenosines. In strand X, the bulged adenosine (X5) is in a C2′ *endo* conformation and is pointing out away from the helix, whereas in strand Y the bulged adenosine (Y5) is more parallel to the helix. The nucleotides opposite the bulge (nt 9 and 10) adopt canonical A-form conformations. In each strand, the torsion angle deviations adjacent to the bulge appear to compensate for the bulged nucleotides allowing the helix to return to an A-form conformation. The fact that the RNA maintains a conformation so similar to A-form through torsion angle deviations despite the bulged nucleotides would suggest that stacking is the dominant structural driving force in this RNA structure.

The effects of the bulged adenosines on base stacking in the RNA helix were evaluated using the program Freehelix (Dickerson, 1998) to determine rise, twist, and inclination for the base pairs. The bulged adenosines were omitted from the duplex for these calculations. The average rise is 2.7 Å per base pair with a range of 2.5 to 3.0 Å per base pair; the average twist is 33.6° with a range of 29.7° to 39.4°; and the average inclination is 15.7° with a range of 11.4° and 19.5°. These average values are very close to those of A-form RNA, which has a rise of 2.8 Å per base pair, a twist of 32.7°, and an inclination of 16°. The closely related A′-form RNA has a rise of 3.0 Å per base pair, a twist of 30.0°, and an inclination of 10.0° (Arnott et al., 1973). Even the base pairs on either side of the bulged nucleotides are very close to the A-form values. The base step flanking X5 has a rise of 2.5 Å, a twist of 39.4°, and inclinations of 15.7° and 11.4°, and the base pairs flanking Y5 have a rise of 2.8 Å, a twist of 36.9°, and inclinations of 13.2° and 15.9°. This analysis shows that although the phosphate backbone is quite flexible and can easily accommodate a bulged nucleotide, base stacking is robust and maintains a conformation that is strikingly similar to A-form RNA. This ability of RNA to incorporate bulges with only local distortions appears to be a common theme, because similar results have been obtained in other duplexes with bulges (Cate et al., 1996; Portmann et al., 1996; Ennifar et al., 1999).

Bulged adenosines

The two bulged adenosines in the structure described here adopt two different orientations. Superposition of the two chains (Fig. 4A) shows that it is only in the region of the bulge that the two chains differ significantly. Nucleotide X5 (aqua) adopts a C2′-*endo* conformation and Y5 (orange) adopts a C3′-*endo* conformation which, together with the differences in torsion angles, places these bulged adenosines in very different orientations although they are embedded in the same BPS–U2 snRNA helix.

The two bulged adenosine conformations observed here were compared with six other RNAs containing bulged adenosines from the P4-P6 domain of a group I ribozyme (Cate et al., 1996), the MS2 stem-loop RNA (Valegard et al., 1994), a stem-loop of a spliced leader RNA (Greenbaum et al., 1996), and an RNA/DNA chimera (Portmann et al., 1996; Fig. 4B,C). In these various structures, the base of the bulged adenosine is observed to be both parallel or perpendicular to the nearby bases in the helix and the sugars adopt several conformations. The bulged adenosines generally do not fold back to interact with the helix except for the bulged adenosine in the NMR structure of a spliced leader RNA, which hydrogen bonds with a 2′ OH of a ribose group in the RNA helix (Greenbaum et al., 1996). In the other structures determined by X-ray crystallography, these bulged adenosines interact with neighboring RNA helices within the crystal lattice, or with protein in the case of the MS2 bulged adenosine (Valegard et al., 1994), which likely stabilizes the specific conformations observed in these structures. Bulged adenosines might otherwise sample many different conformations. Intercalation of bulged adenosines into the RNA helix has also been observed in the NMR structure of the uncomplexed MS2 RNA and in NMR structures of other duplex RNAs (Borer et al., 1995; Smith & Nikonowicz, 1998; Thiviyanathan et al., 2000).

The variety of structures observed for bulged adenosines suggests that they are quite malleable and could be utilized in a variety of ways for RNA tertiary interactions, protein interactions, and RNA chemistry. In the context of the spliceosome, a bulged adenosine acts as a nucleophile, and several RNAs and proteins appear to position the branchsite adenosine in a flipped out position for attack at the 5′ splice site (Query et al., 1994). Although other factors appear to be involved in positioning the branchsite adenosine, it is interesting to note that in our structure, one of the bulged adenosines (Y5, orange) is in a conformation allowing the 2′ OH to interact with a neighboring helix (Fig. 5A). The bulged adenosine of chain X, on the other hand, is oriented so that its 2′ OH is not interacting with another helix and does not appear to be as accessible as the 2′ OH of the Y5 adenosine (Fig. 5B). Even though the 2′OH of the Y5 bulged adenosine in this structure is being used in crystal packing interactions (see next section for details), it is tempting to speculate that an orientation similar to this one would allow the spliceosome to activate this 2′OH for nucleophilic attack.

Crystal packing and RNA tertiary interactions

The RNA helices stack to form long pseudo-continuous helices within the crystal lattice, as commonly occurs in crystals of nucleic acids. However, the lattice interactions between these long, stacked helices are unique. The bulged adenosines from neighboring helices stack on one another and fit tightly into the minor groove of a third helix to form a three helix interaction (Fig. 6).

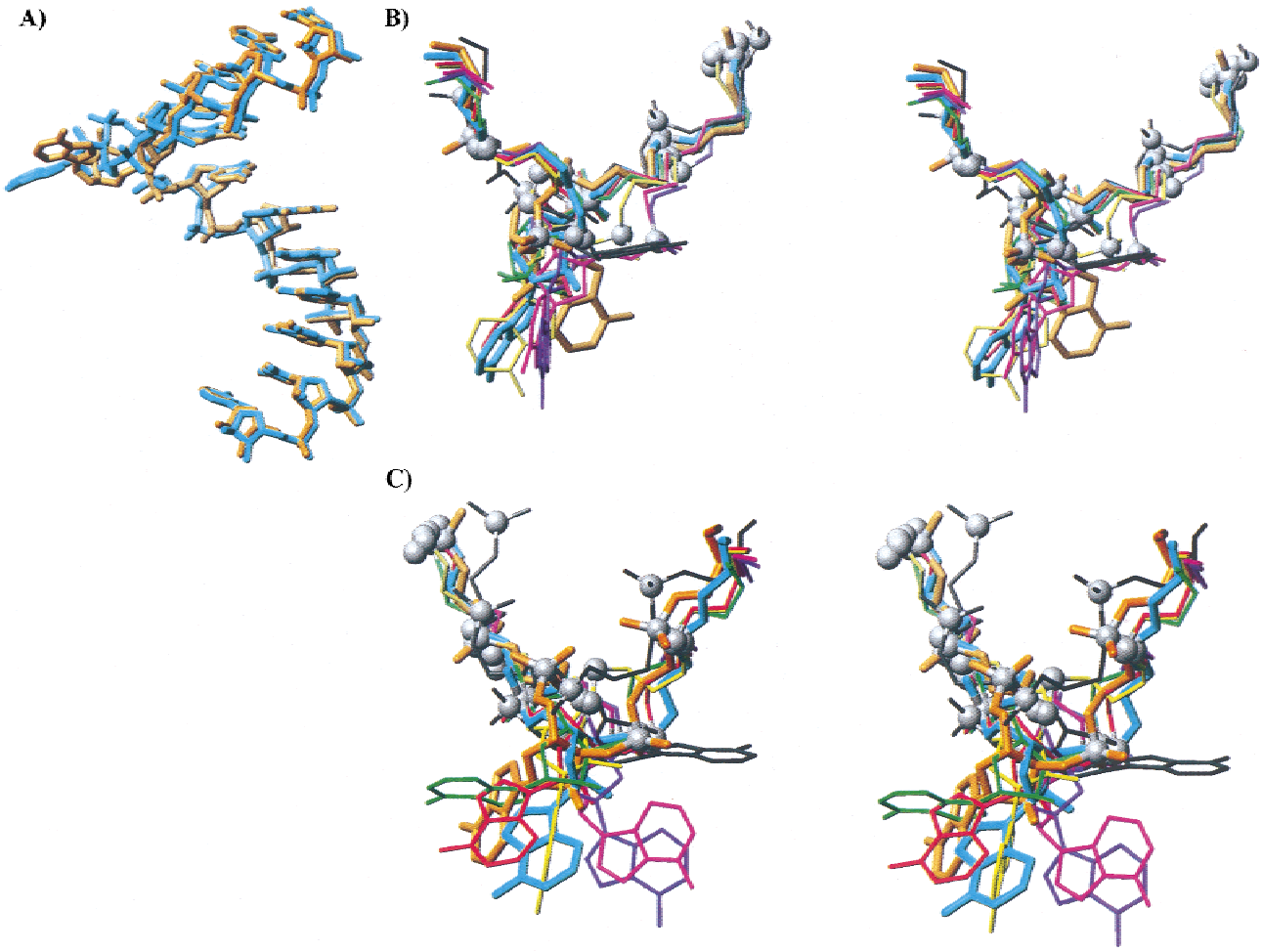

FIGURE 4. Superposition of bulged adenosines. **A:** Comparison of X chain (aqua) and Y chain (orange) by superimposing the two chains. **B:** Superposition of eight bulged adenosines from otherwise Watson–Crick duplex RNA structures shown in stereo. For clarity only the backbones and bulged adenosines for each molecule are shown. Phosphates are shown as silver van der Waal spheres. The bulged adenosines from the structure described here are shown in aqua and orange as previously and are thicker compared to the other bulged adenosines. The other bulged adenosines are two from the P4P6 crystal structure (red and yellow), two from the RNA/DNA chimera crystal structure (fucia and purple), one from the MS2 complex crystal structure (green), and one from the RNA spliced leader NMR structure (black). **C:** The superposition is rotated 90° in comparison to the view in **B** and again shown in stereo.

Seven hydrogen bonds lock the two stacked bulged adenosines into the minor groove of the third helix. The atoms involved in these hydrogen bonds and the distances between appropriate hydrogen bond donor and acceptor groups are listed in Table 2. For clarity each of the three helices will be given a roman numeral for identification (see Fig. 6 and Table 2). Five of the hydrogen bonds involve 2′ OH groups and one of these is a direct 2′ OH–2′ OH hydrogen bond. The bulged X5 (helix I, aqua) adenosine is making two hydrogen bonds to the base (O2) and ribose (2′ OH) groups of the X9 uridine of helix III (Fig. 6C) through its base groups (N1 and N6). The bulged Y5 adenosine (helix II, orange) forms the other five hydrogen bonds via its ribose (2′ OH and 3′ OH) and base (N1 and N3) groups and the ribose (2′ OH) and base groups (N2 and N3) of the X8-Y7 G-C base pair of helix III (gray). Adenosines interacting with the minor groove have been seen before (Portmann et al., 1996; Su et al., 1999), and in the case of the P4-P6 domain, there are three examples in which adenosines interact in the minor groove in a similar fashion as observed for the Y5 adenosine in this structure (Cate et al., 1996). This is the first observation of bulged adenosines being used to form a three-helix interaction.

In addition to direct hydrogen bonding and stacking interactions, two water molecules (W1, W2) bridge the three-helix interaction observed here (Fig. 6A, red spheres). One of these waters, W1, sits above the bulged adenosines and bridges helix II (orange) and helix III (gray) via four hydrogen bonds in a geometry close to tetrahedral. This water (W1) is well ordered in its pocket (Fig. 7) and has a crystallographic B-value that is comparable to those of the surrounding RNA

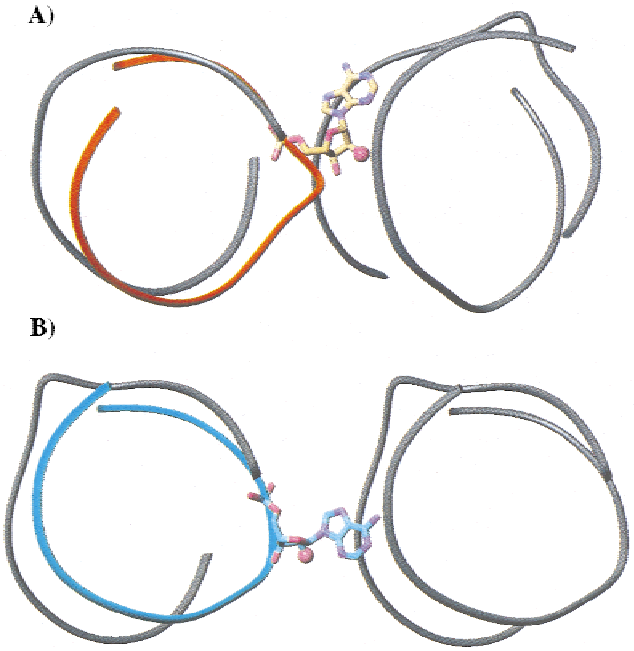

FIGURE 5. Position of the 2′OH in the bulged adenosine RNA structure. **A:** The Y chain is again shown in orange and for clarity only the bulged adenosine (Y5) is shown with everything else being represented by a ribbon through the phosphate backbone. A neighboring helix from the crystal lattice is shown in gray. **B:** As in **A**, only X5 (bulged adenosine) is shown as an all atom representation in aqua. In both **A** and **B**, the 2′ OH is highlighted as a van der Waals sphere and the nitrogen atoms are shown in purple and the oxygen atoms in red.

(35–40 Å^2). W2 also bridges helix II via the N7 group of Y5 (bulged adenosine) and helix III via the 2′ OH group of Y8 (guanosine). These hydrogen bonds are listed in Table 2. The other 20 ordered water molecules in this structure form hydrogen bonds with only one helix.

Although divalent metals frequently mediate RNA packing and tertiary interactions (Laing et al., 1994; Cate et al., 1997; Ennifar et al., 1999), the structure of the bulged adenosine helix described here is free of divalent metal ions, and no ordered monovalent ions appear to be involved in the packing interactions. Crystallization is dependent upon the presence of spermine, but there is no apparent electron density for ordered spermine in this structure, suggesting that it is either disordered or exists at low occupancy. Perhaps RNA tertiary interactions involving bulged nucleotides are less dependent upon the presence of metals than other types of RNA tertiary interactions as they can maintain a greater than usual distance between the phosphate backbones of adjacent helices. The three-helix interaction described here brings the phosphate groups to within 5 Å in one location, but otherwise maintains spacing of greater than 7 Å. The type of three-way RNA interaction described here may provide a generally useful scheme for folding in RNAs by bringing together three helical regions. Crystal packing interactions have previously served as models for relevant tertiary interactions; for example, the hammerhead ribozyme structure (Pley et al., 1994) provided a tetraloop–minor groove interaction that is similar to the now commonly observed tetraloop–tetraloop receptor motif (Costa & Michel, 1995; Cate et al., 1996).

Implications for pre-mRNA splicing and self-splicing Group II RNAs

In the yeast *S. cerevisiae*, the U2 snRNA–BPS is highly conserved in sequence, presenting the possibility that this sequence forms an unusual RNA structure that might explain the nucleophilic character of the branchsite adenosine. In light of our structure, however, this does not appear to be the case because the structure described here is essentially identical to A-form RNA. Although it is possible that when the adjacent adenosine (X6/Y6) is unpaired and flipped out, the RNA adopts a structure that specifically positions this nucleotide for nucleophilic attack, our structure suggests that additional information, from other RNAs or proteins, is required to orient the branchsite adenosine and properly select the correct phosphodiester bond for attack.

TABLE 1. Crystallographic statistics.

Data collection	Native	Iodine-1	Iodine-2
Resolution (Å)	2.18	2.2	2.9
Unit cell			
Space group	$P2_1$	$P2_1$	$P2_1$
a (Å)	28.75	28.90	28.84
B (Å)	42.40	42.72	42.56
c (Å)	33.14	33.34	33.17
β (°)	92.87	92.10	92.77
Total observations	20,240	9040	3716
Unique observations	4125	3885	1752
Intensity/σIntensity	13,820/460	11,035/1334	2620/315
(Last shell)	(245/94)	(365/209)	(340/131)
Completeness	96	93	92
(Last shell)	(94)	(96)	(88)
R_{sym}	0.048	0.089	0.095
(Last shell)	(0.38)	(0.49)	(0.34)
R_{iso}	—	0.30	0.23
R_{cullis}	—	0.66	0.47
Phasing power	—	1.49	1.80
Occupancy	—	1.09 0.92	0.72 0.71
Asymmetric unit	1 duplex	1 duplex	1 duplex
Model refinement			
Resolution limits (Å)	8–2.18		
Data selected	All		
Bulk solvent mask	No		
$R_{crystal}$	25.3%		
R_{free} (10%)	27.6%		
Average B value	58 Å		
Waters in the model	22		

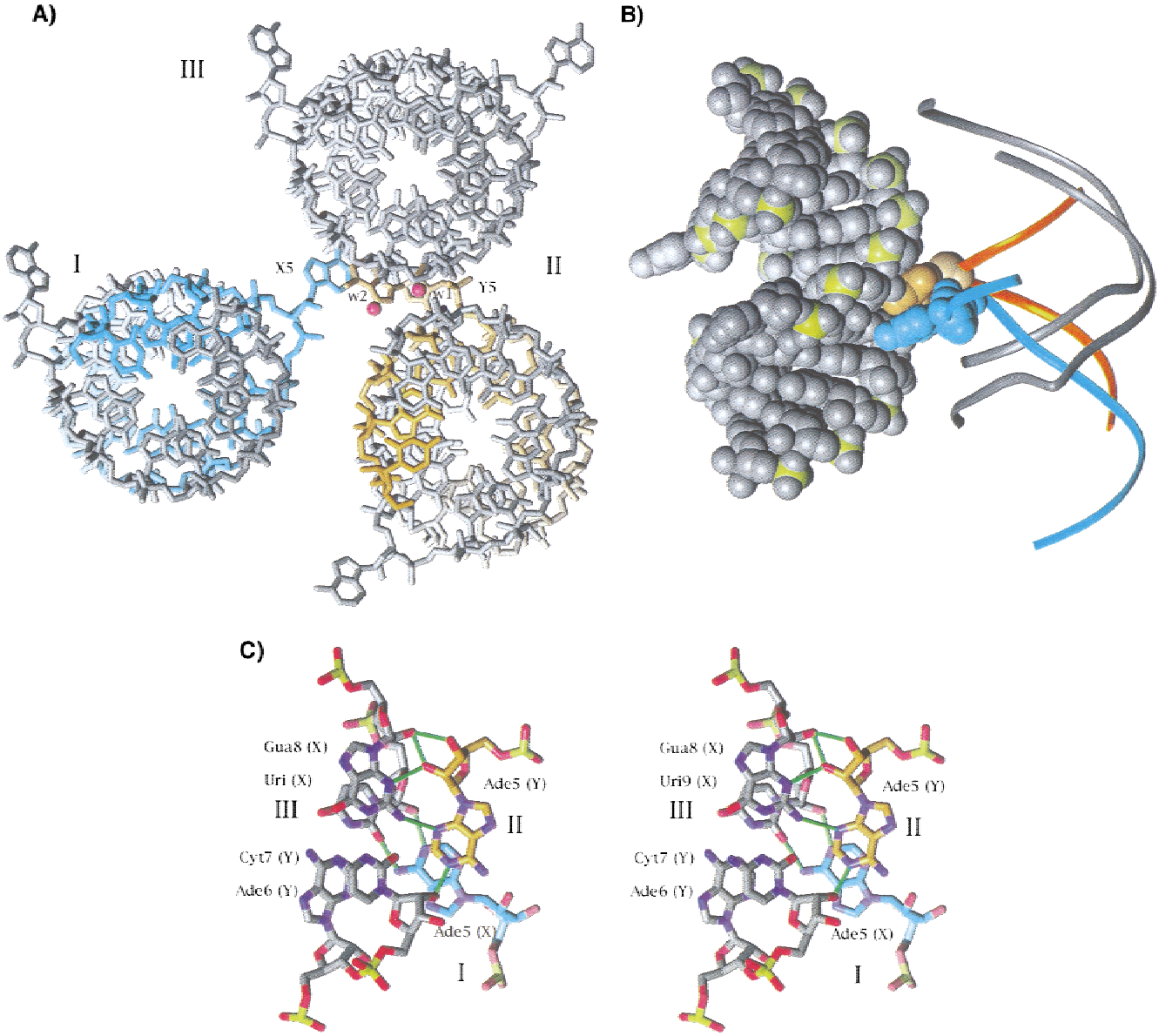

FIGURE 6. RNA tertiary interactions revealed by crystal packing. **A:** The packing observed in the crystals as viewed down the helical axis (C axis of the unit cell) of the RNA. For clarity the three different helices are labeled with roman numerals, helix I contains the X5 bulged adenosine shown in aqua, helix II contains the Y5 bulged adenosine shown in orange and helix III is shown in gray. Three red spheres represent the waters (W1, W2) at the three helix interface. **B:** This view is rotated 90° from the view in **A**. The bulged adenosines and the adjacent helix are shown in a van der Waals representation to demonstrate the packing interaction occurring at this interface. For clarity the other two helices are shown as ribbons. Phosphates are shown in yellow in helix III. **C:** Stereo view showing the bulged adenosines interacting in the minor groove of the adjacent helix. Only the two bulged adenosines (X5: helix I, Y5: helix II) and two base pairs (X8 guanosine base paired with the Y7 cytosine and X9 uridine base paired with the Y6 adenosine) from helix III are shown. The amino groups are shown in blue and the oxygen groups in red. The hydrogen bonds are shown as green lines.

The crystal packing interactions described here shed light on how the spliceosomal RNAs and proteins might position the branchsite adenosine for nucleophilic attack through base stacking and hydrogen bond interactions. A bulged adenosine is also an important element in self-splicing group II RNAs in that it also acts as the branchsite nucleophile in the first step of catalysis and is found unpaired in a helical region of the RNA termed domain VI (Qin & Pyle, 1998). Recently it has been shown that domain VI is in contact with domain V, another critical helical element of group II introns (Podar & Perlman, 1999). Domains V and VI also interact with the 5′ splice site, which is in yet another helical region. Perhaps a three helix interaction similar to the one described here could be involved in defining the catalytic site during the first step in the self-splicing group II RNA reaction.

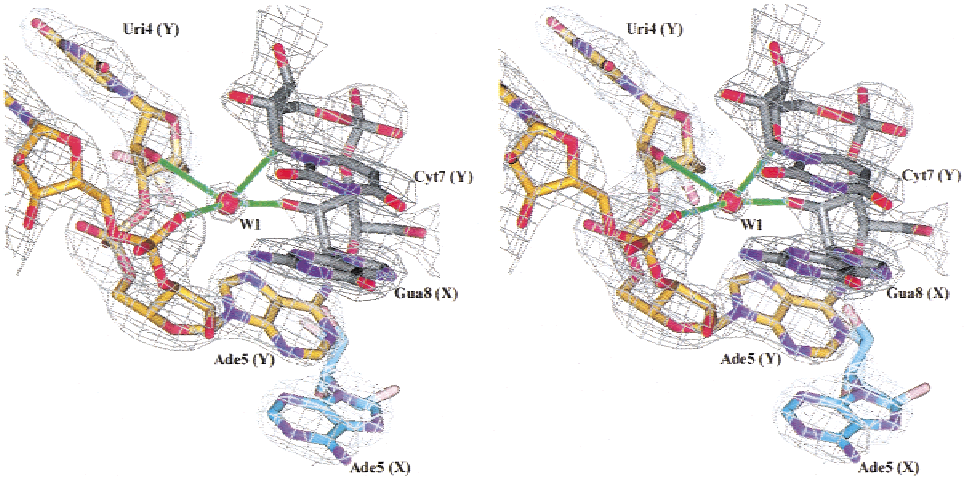

FIGURE 7. A bridging water in the three helix RNA interaction. The color scheme is the same as in previous figures. The map shown in dark gray is an omit map at 1.6 sigma. This water (W1, red) is making four hydrogen bonds between helices II and III (details are in Table 2), which are shown in green.

MATERIALS AND METHODS

RNA synthesis, purification, and crystallization

The RNA (UACUAACGUAGUA) was synthesized using Perseptive Expedite RNA amidites on an Expedite 8909 Oligonucleotide Synthesizer or by Dharmacon Research, Inc. (Boulder, Colorado). No differences were observed in crystallization of RNAs from these two different sources. RNAs were deprotected as recommended by their respective manufacturers and purified using a Nucleopac PA-100 anion exchange HPLC column (Dionex) equilibrated in 25 mM Tris (pH 8.0), 0.5% Acetonitrile, and 240 mM NH_4Cl and heated to 85 °C. A gradient of NH_4Cl (100–800 mM) was used to elute the RNA. Peak fractions were concentrated using an Amicon Flow cell, twice precipitated with ethanol, and then dried and resuspended in 1/10 TE. Vapor diffusion using the hanging drop method was employed to crystallize the RNA. RNA at a concentration of 2–5 mg/mL was mixed in a 1:1 ratio with well solution containing 10% 2-methyl-2,4-pentanediol (MPD), 10–25% glycerol, 25 mM Tris (pH 7.5) and 1–3 mM spermine and then equilibrated against 1 mL of well solution at 30 °C for 1 day and then at 14 °C for several more days. Crystals obtained maximum size within one week.

Data collection, structure determination, and refinement

Native and derivative data were collected from crystals (mounted directly from crystallization drops) at room temperature using an R-AXIS IIC detector and a Rigaku RU-H2R rotating anode generator equipped with the MSC/Yale design focusing mirrors (Molecular Structure Corp., The Woodlands, Texas). Although crystallization conditions (presence of MPD and glycerol) were optimal for freezing, the mosaicity was always high, precluding the use of this data for structure determination. Data were reduced to reflection intensities using DENZO and SCALEPACK (Otwinowski & Minor, 1997). Space group, unit cell parameters, and the data reduction statistics are listed in Table 1. The structure was solved using multiple heavy atom isomorphous replacement (MIR) using two 5-iodouridine substituted RNAs (at positions 1 and 9). The iodine positions were identified by inspection of difference Patterson maps and by difference Fourier methods (Collaborative Computational Project, 1994) and then refined using MLPHARE (Otwinowski, 1991). The heavy atom refinement statistics are listed in Table 1. After density modification using the program DM (Cowtan & Main, 1998), the electron density maps were of sufficient quality to build in 4 bp on either end of the helix and also the uridines at positions 1 and 9 using O (Jones et al., 1991). These nucleotides were refined as individual rigid bodies using CNS (Brunger et al., 1998), and combined electron density maps were then generated using phases calculated from these coordinates together with the experimental phases (phase combination). The remainder of the molecule (except the bulged adenosines) was then fit into

TABLE 2. Hydrogen bonds at the three-helix interface.

Helix I (aqua)	Helix II (orange)	Helix III (gray)	Bridging H_2O	Distance (Å)
N6 Ade X5		O2 Uri X9		2.90
N1 Ade X5		2′OH Uri X9		2.67
	N1 Ade Y5	2′OH Cyt Y7		2.61
	N3 Ade Y5	N2 Gua X8		3.08
	2′OH Ade Y5	2′OH Gua X8		2.52
	2′OH Ade Y5	N3 of Gua X8		2.73
	3′OH Ade Y5	2′OH Gua X8		3.05
	2′OH Uri Y4		W1	3.20
	O2P Ade Y6		W1	2.57
		2′OH Gua Y8	W1	2.58
		04′ Uri Y9	W1	3.18
	N7 Ade Y5		W2	3.15
		2′OH Gua Y8	W2	3.15

For orientation within the helix, X8 guanosine is base paired to the Y7 cytosine.

these combined maps. After another round of rigid body refinement in CNS, the bulged adenosines were added and several rounds of manual refitting and positional refinement were carried out using O and CNS. Water molecules were introduced into 2Fo–Fc electron density if they were within hydrogen bonding distance of an appropriate hydrogen bond donor or acceptor group on the RNA. Currently, $R_{free} = 27.6\%$ (10% of data) and $R_{crystal} = 25.3\%$.

Accession numbers

The atomic coordinates and structure factors for the BPS–U2 snRNA duplex have been deposited in the Nucleic Acid Database with accession number 1I9X.

ACKNOWLEDGMENTS

We thank members of the Schultz lab for their advice and suggestions during this work. We are grateful to Martin Horvath, Olve Peersen, Dan Harrington, and Tom Cech for their critical reading of the manuscript. We are indebted to an anonymous reviewer for pointing out a ribose with incorrect chirality. We also would like to thank Carolyn Kotarski for RNA synthesis. This work was funded in part by a Colorado RNA Center grant. J.A.B. is Burroughs Wellcome Fund Fellow of the Life Sciences Research Foundation.

Received October 25, 2000; returned for revision November 8, 2000; revised manuscript received January 22, 2001

REFERENCES

Adema GJ, Bovenberg RA, Jansz HS, Baas PD. 1988. Unusual branch point selection involved in splicing of the alternatively processed Calcitonin/CGRP-I pre-mRNA. *Nucleic Acids Res 16*:9513–9526.

Arning S, Gruter P, Bilbe G, Kramer A. 1996. Mammalian splicing factor SF1 is encoded by variant cDNAs and binds to RNA. *RNA 2*:794–810.

Arnott S, Hukins DW, Dover SD, Fuller W, Hodgson AR. 1973. Structures of synthetic polynucleotides in the A-RNA and A′-RNA conformations: X-ray diffraction analyses of the molecular conformations of polyadenylic acid–polyuridylic acid and polyinosinic acid–polycytidylic acid. *J Mol Biol 81*:107–122.

Berglund JA, Chua K, Abovich N, Reed R, Rosbash M. 1997. The splicing factor BBP interacts specifically with the pre-mRNA branchpoint sequence UACUAAC. *Cell 89*:781–787.

Borer PN, Lin Y, Wang S, Roggenbuck MW, Gott JM, Uhlenbeck OC, Pelczer I. 1995. Proton NMR and structural features of a 24-nucleotide RNA hairpin. *Biochemistry 34*:6488–6503.

Brunger AT, Adams PD, Clore GM, DeLano WL, Gros P, Grosse-Kunstleve RW, Jiang JS, Kuszewski J, Nilges M, Pannu NS, Read RJ, Rice LM, Simonson T, Warren GL. 1998. Crystallography & NMR system: A new software suite for macromolecular structure determination. *Acta Crystallogr D Biol Crystallogr 54*:905–921.

Burge CB, Tuschl T, Sharp PA. 1999. Splicing of precursors to mRNAs by the spliceosomes. In: Gesteland RF, Cech TR, Atkins F, eds. *The RNA world*, 2nd ed. Cold Spring Harbor, New York: Cold Spring Harbor Laboratory Press. pp 525–560.

Cate JH, Gooding AR, Podell E, Zhou K, Golden BL, Kundrot CE, Cech TR, Doudna JA. 1996. Crystal structure of a group I ribozyme domain: Principles of RNA packing. *Science 273*:1678–1685.

Cate JH, Hanna RL, Doudna JA. 1997. A magnesium ion core at the heart of a ribozyme domain. *Nat Struct Biol 4*:553–558.

Chiara MD, Gozani O, Bennett M, Champion-Arnaud P, Palandjian L, Reed R. 1996. Identification of proteins that interact with exon sequences, splice sites, and the branchpoint sequence during each stage of spliceosome assembly. *Mol Cell Biol 16*:3317–3326.

Collaborative Computational Project. 1994. The CCP4 suite: Programs for protein crystallography. *Acta Cryst D50*:760–763.

Costa M, Michel F. 1995. Frequent use of the same tertiary motif by self-folding RNAs. *EMBO J 14*:1276–1285.

Cowtan K, Main P. 1998. Miscellaneous algorithms for density modification. *Acta Crystallogr D 54*:487–493.

Dickerson RE. 1998. DNA bending: The prevalence of kinkiness and the virtues of normality. *Nucleic Acids Res 26*:1906–1926.

Dyhr-Mikkelsen H, Kjems J. 1995. Inefficient spliceosome assembly and abnormal branch site selection in splicing of an HIV-1 transcript in vitro. *J Biol Chem 270*:24060–24066.

Ennifar E, Yusupov M, Walter P, Marquet R, Ehresmann B, Ehresmann C, Dumas P. 1999. The crystal structure of the dimerization initiation site of genomic HIV-1 RNA reveals an extended duplex with two adenine bulges. *Structure Fold Des 7*:1439–1449.

Ferre-D'Amare AR, Doudna JA. 1999. RNA folds: Insights from recent crystal structures. *Annu Rev Biophys Biomol Struct 28*:57–73.

Greenbaum NL, Radhakrishnan I, Patel DJ, Hirsh D. 1996. Solution structure of the donor site of a trans-splicing RNA. *Structure 4*:725–733.

Gutell RR, Weiser B, Woese CR, Noller HF. 1985. Comparative anatomy of 16-S-like ribosomal RNA. *Prog Nucleic Acid Res Mol Biol 32*:155–216.

Hartmuth K, Barta A. 1988. Unusual branch point selection in processing of human growth hormone pre-mRNA. *Mol Cell Biol 8*:2011–2020.

Jones TA, Zou JY, Cowan SW, Kjeldgaard M. 1991. Improved methods for building protein models in electron density maps and the location of errors in these models. *Acta Crystallogr A 47*:110–119.

Laing LG, Gluick TC, Draper DE. 1994. Stabilization of RNA structure by Mg ions. Specific and non-specific effects. *J Mol Biol 237*:577–587.

MacMillan AM, Query CC, Allerson CR, Chen S, Verdine GL, Sharp PA. 1994. Dynamic association of proteins with the pre-mRNA branch region. *Genes & Dev 8*:3008–3020.

Nilsen TW. 1998. RNA–RNA interactions in nuclear pre-mRNA splicing. In: Simons RW, Grungerg-Manago M, eds. *RNA structure and function.* Cold Spring Harbor, New York: Cold Spring Harbor Laboratory Press. pp 279–308.

Otwinowski Z. 1991. Maximum likelihood refinement of heavy atom parameters. In: Wolf W, Evans PR, Leslie AGW, eds. *Isomorphous replacement and anomalous scattering*. Daresbury, UK: Daresbury Laboratory. pp 80–85.

Otwinowski Z, Minor W. 1997. Processing of X-ray diffraction data collected in oscillation mode. *Methods Enzymol 276*:307–326.

Parker R, Siliciano PG, Guthrie C. 1987. Recognition of the TACTAAC box during mRNA splicing in yeast involves base pairing to the U2-like snRNA. *Cell 49*:229–239.

Perrotta AT, Nikiforova O, Been MD. 1999. A conserved bulged adenosine in a peripheral duplex of the antigenomic HDV self-cleaving RNA reduces kinetic trapping of inactive conformations. *Nucleic Acids Res 27*:795–802.

Pley HW, Flaherty KM, McKay DB. 1994. Model for an RNA tertiary interaction from the structure of an intermolecular complex between a GAAA tetraloop and an RNA helix. *Nature 372*:111–113.

Podar M, Perlman PS. 1999. Photocrosslinking of 4-thio uracil-containing RNAs supports a side-by-side arrangement of domains 5 and 6 of a group II intron. *RNA 5*:318–329.

Portmann S, Grimm S, Workman C, Usman N, Egli M. 1996. Crystal structures of an A-form duplex with single-adenosine bulges and a conformational basis for site-specific RNA self-cleavage. *Chem Biol 3*:173–184.

Qin PZ, Pyle AM. 1998. The architectural organization and mechanistic function of group II intron structural elements. *Curr Opin Struct Biol 8*:301–308.

Query CC, Moore MJ, Sharp PA. 1994. Branch nucleophile selection in pre-mRNA splicing: Evidence for the bulged duplex model. *Genes & Dev 8*:587–597.

Query CC, Strobel SA, Sharp PA. 1996. Three recognition events at the branch-site adenine. *EMBO J 15*:1392–1402.

Ruskin B, Pikielny CW, Rosbash M, Green MR. 1986. Alternative branch points are selected during splicing of a yeast pre-mRNA in

mammalian and yeast extracts. *Proc Natl Acad Sci USA 83*:2022–2026.
Ruskin B, Zamore PD, Green MR. 1988. A factor, U2AF, is required for U2 snRNP binding and splicing complex assembly. *Cell 52*: 207–219.
Rutz B, Séraphin B. 1999. Transient interaction of BBP/ScSF1 and Mud2 with the splicing machinery affects the kinetics of spliceosome assembly. *RNA 5*:819–831.
Rymond BC, Rosbash M. 1992. Yeast pre-mRNA splicing. In: Jones EW, Pringle JR, Broach JR, eds. *The molecular and cellular biology of the yeast Saccharomyces: Gene expression*. Cold Spring Harbor, New York: Cold Spring Harbor Laboratory Press. pp 143–192.
Smith JS, Nikonowicz EP. 1998. NMR structure and dynamics of an RNA motif common to the spliceosome branch-point helix and the RNA-binding site for phage GA coat protein. *Biochemistry 37*: 13486–13498.
Spingola M, Grate L, Haussler D, Ares M Jr. 1999. Genome-wide bioinformatic and molecular analysis of introns in *Saccharomyces cerevisiae*. *RNA 5*:221–234.
Staley JP, Guthrie C. 1998. Mechanical devices of the spliceosome: Motors, clocks, springs, and things. *Cell 92*:315–326.
Su L, Chen L, Egli M, Berger JM, Rich A. 1999. Minor groove RNA triplex in the crystal structure of a ribosomal frameshifting viral pseudoknot. *Nat Struct Biol 6*:285–292.
Thiviyanathan V, Guliaev AB, Leontis NB, Gorenstein DG. 2000. Solution conformation of a bulged adenosine base in an RNA duplex by relaxation matrix refinement. *J Mol Biol 300*:1143–1154.
Valcarcel J, Gaur RK, Singh R, Green MR. 1996. Interaction of U2AF65 RS region with pre-mRNA branch point and promotion of base pairing with U2 snRNA. *Science 273*:1706–1709.
Valegard K, Murray JB, Stockley PG, Stonehouse NJ, Liljas L. 1994. Crystal structure of an RNA bacteriophage coat protein-operator complex. *Nature 371*:623–626.
Wu J, Manley JL. 1989. Mammalian pre-mRNA branch site selection by U2 snRNP involves base pairing. *Genes & Dev 3*:1553–1561.
Zabolotny JM, Krummenacher C, Fraser NW. 1997. The herpes simplex virus type 1 2.0-kilobase latency-associated transcript is a stable intron which branches at a guanosine. *J Virol 71*:4199–4208.
Zhuang Y, Weiner AM. 1989. A compensatory base change in human U2 snRNA can suppress a branch site mutation. *Genes & Dev 3*:1545–1552.